*Inorg. Chem.* **2009**, *48*, 331−338

# Stability of the Heme Fe−N-Terminal Amino Group Coordination Bond in Denatured Cytochrome *c*

**Hulin Tai,[†] Toratane Munegumi,[‡] and Yasuhiko Yamamoto*[,†]**

*Department of Chemistry, University of Tsukuba, Tsukuba 305-8571, Japan, and Department of Materials Chemistry and Bioengineering, Oyama National College of Technology, Oyama, Tochigi 323-0806, Japan*

Received June 30, 2008

In the denatured states of *Hydrogenobacter thermophilus* cytochrome $c_{552}$ (HT) and *Pseudomonas aeruginosa* cytochrome $c_{551}$ (PA), and their mutants, the N-terminal amino group of the polypeptide chain is coordinated to heme Fe in place of the axial Met, the His−$N_{term}$ form being formed. The coordination of the N-terminal amino group to heme Fe leads to loop formation by the N-terminal stretch preceding the first Cys residue bound to the heme, and the N-terminal stretches of HT and PA are different from each other in terms of both the sequence and the number of constituent amino acid residues. The His−$N_{term}$ form was shown to be rather stable, and hence it can influence the stability of the denatured state. We have investigated the heme Fe coordination structures and stabilities of the His−$N_{term}$ forms emerging upon guanidine hydrochloric acid-induced unfolding of the oxidized forms of the proteins. The Fe−$N_{term}$ coordination bond in the His−$N_{term}$ form with a 9-residue N-terminal stretch of HT proteins was found to be tilted to some extent away from the heme normal, as reflected by the great heme methyl proton shift spread. On the other hand, the small heme methyl proton shift spread of the His−$N_{term}$ form with an 11-residue stretch of PA proteins indicated that its Fe−$N_{term}$ bond is nearly parallel with the heme normal. The stability of the His−$N_{term}$ form was found to be affected by the structural properties of the N-terminal stretch, such as its length and the N-terminal residue. With a given N-terminal residue, the stability of the His−$N_{term}$ form is higher for a 9-residue N-terminal stretch than an 11-residue one. In addition, with a given length of the N-terminal stretch, the His−$N_{term}$ form with an N-terminal Glu is stabilized by a few kJ $mol^{-1}$ relative to that with an N-terminal Asn. These results provide a novel insight into the stabilizing interactions in the denatured cyts *c* that will facilitate elucidation of the folding/unfolding mechanisms of the proteins.

## Introduction

Understanding the molecular mechanisms of protein folding and unfolding remains one of the most challenging tasks in life sciences. It requires not only detailed knowledge of various species, transient or long-lived, involved in folding/unfolding reactions, but also detailed kinetic information that connects these species. Early work on protein folding assumed that the denatured state of a protein is devoid of any persistent structure, and hence the protein polypeptide chain was considered to be a random coil.[1] Nowadays, however, it is widely accepted that protein-denatured states can contain somewhat ordered structures known as residual structures.[2] These structures have been shown to persist even under highly denaturing conditions[3−8] and are likely an important factor in protein folding.[3,4] Such residual structures can significantly influence the energy of the denatured state.[9]

The class I cytochromes *c* (cyts *c*) have long served as typical models for examination of protein folding/unfolding. Cyt *c* is a hemoprotein and contains a single heme covalently bound to a polypeptide chain. His and Met residues are coordinated to heme Fe as axial ligands in the native state.[10,11] However, upon unfolding of the protein, several different heme coordination structures have been de-

* To whom correspondence should be addressed. Phone/Fax: +81 29 853 6521. E-mail: yamamoto@chem.tsukuba.ac.jp.
† University of Tsukuba.
‡ Oyama National College of Technology.

(1) Tanford, C. *Adv. Protein Chem.* **1968**, *23*, 121–282.
(2) Fleming, P. J.; Rose, G. D. *Protein Folding Handbook, Part I: Conformational properties of unfolded proteins*; Buchner, J., Kiefhaber, T., Eds.; Wiley-VCH: Weinheim, Germany, 2005; pp 710−736.
(3) Dill, K.; Shortle, D. *Annu. Rev. Biochem.* **1991**, *60*, 795–825.
(4) Shortle, D. *Curr. Opin. Struct. Biol.* **1996**, *6*, 24–30.

10.1021/ic801202d CCC: $40.75 
Published on Web 11/21/2008

tected.[12−42] These nonnative heme coordination structures of cyt *c* have been recognized as important intermediates of protein folding/unfolding, and hence detailed characterization of their structures and stabilities is valuable for understanding the protein folding mechanism.

**Scheme 1.** pH Dependence of the Heme Coordination Structure in the Denatured Cyt *c* Possessing a Single His Residue As an Axial Ligand for Heme Fe and Non-acetylated N-Terminal Amino Group

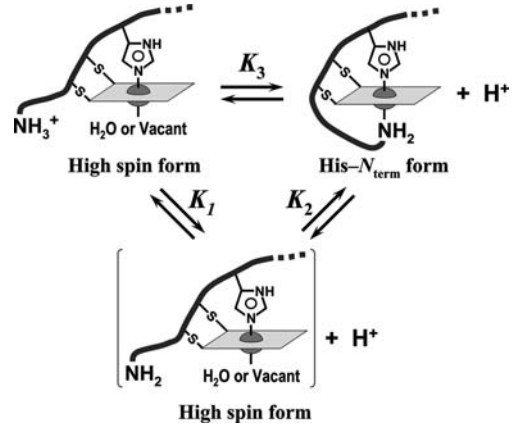


In the cyt *c* protein scaffold, particularly in the case of oxidized cyt *c*, Fe-bound Met is more susceptible to displacement under nonnative conditions, compared with Fe-bound His, which remains in close proximity to the heme. Cleavage of the native Fe−Met bond in oxidized cyt *c* is thought to accompany the first step of protein unfolding under various nonnative conditions.[12,14,23,24] In the case of cyt *c* possessing a single His residue as an axial ligand for heme Fe, together with non-acetylated N-terminal amino group, the N-terminal amino group of the polypeptide chain has been shown to act as an axial ligand for heme Fe in place of the axial Met of the denatured protein, the His−$N_{term}$ form being formed (see Supporting Information).[24,30,33−37] The coordination of the N-terminal amino group to heme Fe leads to loop formation by the N-terminal stretch preceding the first Cys residue bound to the heme. As illustrated in Scheme 1, the His−$N_{term}$ form is stable at neutral pH and, as the pH decreases, the N-terminal amino group is protonated and hence the Fe−$N_{term}$ bond is broken. Since cleavage of the Fe−$N_{term}$ bond accompanies a change in the spin state of heme Fe, this process can be readily and sensitively detected through observation of the Soret absorption band and hence the equilibrium constant $K_3$ in Scheme 1 is yielded by fitting of the data to the Henderson−Hasselbalch equation.[33−36,44] This equilibrium can be represented by a two-step process, i.e., deprotonation of the N-terminal amino group and the formation of the Fe−$N_{term}$ bond, which can be assessed on the basis of the equilibrium constants $K_1$ and $K_2$, respectively. Since $K_1$ can be estimated through the study of an appropriate model peptide, the $K_2$ value, which directly reflects the stability of the Fe−$N_{term}$ bond, can be determined through $K_2 = 1 + (K_3/K_1)$.[45]

In this study, we have characterized the stability of the Fe−$N_{term}$ bond of His−$N_{term}$ forms emerging upon guanidine hydrochloric acid (GdnHCl)-induced unfolding of the oxidized forms of *Hydrogenobacter thermophilus* cytochrome


(5) Bond, C. J.; Wong, K.; Clarke, J.; Fersht, A. R.; Daggett, V. *Proc. Natl. Acad. Sci. U.S.A.* **1997**, *94*, 13409–13413.
(6) Shortle, D.; Ackerman, M. S. *Science* **2001**, *293*, 487–489.
(7) Klein-Seetharaman, J.; Oikawa, M.; Grimshaw, S. B.; Wirmer, J.; Duchardt, E.; Ueda, T.; Imoto, T.; Smith, L. J.; Dobson, C. M.; Schwalbel, H. *Science* **2002**, *295*, 1719–1722.
(8) Kohn, J. E.; Millett, I. S.; Jacob, J.; Zagrovic, B.; Dillon, T. M.; Cingel, N.; Dothager, R. S.; seifert, S.; Thiyagarajan, P.; Sosnick, T. R.; Hasan, M. Z.; Pande, V. S.; Ruczinski, I.; Doniach, S.; Plaxco, K. W. *Proc. Natl. Acad. Sci. U.S.A.* **2004**, *101*, 12491–12496.
(9) Bowler, B. E. *Mol. BioSyst.* **2007**, *3*, 88–99.
(10) Moore, G. R.; Pettigrew, G. W. *Cytochromes c: Evolutionary, Structural, and Physicochemical Aspects*; Springer: Berlin, 1990.
(11) Scott, R. A.; Mauk, A. G. *Cytochrome c: A multidisciplinary approach*; University Science Books: Sausalito, CA, 1996.
(12) Roder, H.; Elöve, G. A.; England, S. W. *Nature* **1988**, *335*, 700–704.
(13) Sosnick, T. R.; Mayne, L.; England, S. W. *Nat. Struct. Biol.* **1994**, *1*, 149–156.
(14) Bai, Y.; Sosnick, T. R.; Mayne, L.; England, S. W. *Science* **1995**, *269*, 192–197.
(15) Xu, Y.; Mayne, L.; England, S. W. *Nat. Struct. Biol.* **1998**, *5*, 774–778.
(16) Gianni, S.; Travaglini-Allocatelli, C.; Cutruzzolà, F.; Bigotti, M. G.; Brunori, M. *J. Mol. Biol.* **2001**, *309*, 1177–1187.
(17) Gianni, S.; Travaglini-Allocatelli, C.; Cutruzzolà, F.; Brunori, M.; Shastry, M. C. R.; Roder, H. *J. Mol. Biol.* **2003**, *330*, 1145–1152.
(18) Yeh, S.-R.; Rousseau, D. L. *J. Biol. Chem.* **1999**, *274*, 17853–17859.
(19) Takahashi, S.; Yeh, S.-R.; Das, T. K.; Chan, C.-K.; Gottfriend, D. S.; Rousseau, D. L. *Nat. Struct. Biol.* **1997**, *4*, 44–50.
(20) Bartalesi, I.; Bertini, I.; Ghosh, K.; Rosato, A.; Turano, P. *J. Mol. Biol.* **2002**, *321*, 693–701.
(21) Chevance, S.; Rumeur, E. L.; de Certaines, J. D.; Simonneaux, G.; Bondon, A. *Biochemistry* **2003**, *42*, 15342–15351.
(22) Bertini, I.; Turano, P.; Vasos, P. R.; Bondon, A.; Chevance, S.; Simonneaux, G. *J. Mol. Biol.* **2004**, *336*, 489–496.
(23) Tai, H.; Nagatomo, S.; Mita, H.; Sambongi, Y.; Yamamoto, Y. *Bull. Chem. Soc. Jpn.* **2005**, *78*, 2019–2025.
(24) Tai, H.; Kawano, S.; Yamamoto, Y. *J. Biol. Inorg. Chem.* **2008**, *13*, 25–34.
(25) Russell, B. S.; Melenkivitz, R.; Bren, K. L. *Proc. Natl. Acad. Sci. U.S.A.* **2000**, *97*, 8312–8317.
(26) Russell, B. S.; Bren, K. L. *J. Biol. Inorg. Chem.* **2002**, *7*, 909–916.
(27) Banci, L.; Bertini, I.; Spyroulias, G. A.; Turano, P. *Eur. J. Inorg. Chem.* **1998**, *5*, 583–591.
(28) Berners-Price, S. J.; Bertini, I.; Gray, H. B.; Spyroulias, G. A.; Turano, P. *J. Inorg. Biochem.* **2004**, *98*, 814–823.
(29) Assfaig, M.; Bertini, I.; Dolfi, A.; Turano, P.; Mauk, A. G.; Rosell, F. I.; Gray, H. B. *J. Am. Chem. Soc.* **2003**, *125*, 2913–2922.
(30) Godbole, S.; Dong, A.; Garbin, K.; Bowler, B. E. *Biochemistry* **1997**, *36*, 119–126.
(31) Godbole, S.; Bowler, B. E. *Biochemistry* **1999**, *38*, 487–495.
(32) Nelson, C. J.; Bowler, B. E. *Biochemistry* **2000**, *39*, 13584–13594.
(33) Hammack, B.; Godbole, S.; Bowler, B. E. *J. Mol. Biol.* **1998**, *275*, 719–724.
(34) Godbole, S.; Hammack, B.; Bowler, B. E. *J. Mol. Biol.* **2000**, *296*, 217–228.
(35) Kurchan, E.; Toder, H.; Bowler, B. E. *J. Mol. Biol.* **2005**, *353*, 730–743.
(36) Tzul, F. O.; Kurchan, E.; Bowler, B. E. *J. Mol. Biol.* **2007**, *371*, 577–584.
(37) Rumbley, J. N.; Hoang, L.; Englander, S. W. *Biochemistry* **2002**, *41*, 13894–13901.
(38) Elöve, G. A.; Bhuyan, A. K.; Roder, H. *Biochemistry* **1994**, *33*, 6925–6935.
(39) Colón, W.; Elöve, G. A.; Wakem, L. P.; Sherman, F.; Roder, H. *Biochemistry* **1996**, *35*, 5538–5549.
(40) Colón, W.; Wakem, L. P.; Sherman, F.; Roder, H. *Biochemistry* **1997**, *36*, 12535–12541.
(41) Telford, J. R.; Tezcan, F. A.; Gray, H. B.; Winkler, J. R. *Biochemistry* **1999**, *38*, 1944–1949.
(42) Yeh, S.-R.; Takahashi, S.; Fan, B.; Rousseau, D. L. *Nat. Struct. Biol.* **1997**, *4*, 51–56.
(43) Yeh, S.-R.; Rousseau, D. L. *Nat. Struct. Biol.* **1998**, *5*, 222–228.
(44) Wandschneider, E.; Bowler, B. E. *J. Mol. Biol.* **2004**, *339*, 185–197.
(45) Davis, L. A.; Schejter, A.; Hess, G. P. *J. Biol. Chem.* **1974**, *249*, 2624–2632.

$c_{552}$[46] (HT) and *Pseudomonas aeruginosa* cytochrome $c_{551}$[47] (PA), and selected mutants (see below). HT and PA are composed of 80 and 82 amino acid residues, with N-terminal stretches of NEQLAKQKG and EDPEVLFKNKG, respectively, and exhibit 56% sequence homology with each other. Since HT and PA each possess a single His residue as an axial ligand for heme Fe, both unfolding and refolding of the proteins proceed in the absence of the well-characterized nonnative *bis*-His form,[25,26,30−32,34−43] in which another His side chain is coordinated to heme Fe in place of the axial Met of the denatured state of various cyts *c*. Characterization of GdnHCl-induced unfolding of oxidized HT under physiological pH conditions revealed the formation of the His−$N_{term}$ form.[24] Furthermore, characterization of GdnHCl-induced unfolding of the oxidized form of a mutant, in which the N-terminal Asn of HT is replaced by His (HT-N1H mutant) demonstrated that the His−$N_{term}$ form exhibits almost comparable stability to that of the *bis*-His form (see Supporting Information).[24] In order to determine the effects of the N-terminal amino acid residue on the stability of the His−$N_{term}$ form, we carried out mutual mutation of the N-terminal residue, i.e., N1E and E1N mutations of HT and PA, respectively. In addition, an HT mutant (HT-2GG3), which possesses two extra Gly residues between E2 and Q3, i.e., the N-terminal stretch of this mutant was changed to NEGGQLAKQKG, was also prepared in order to examine the effect of the length of the N-terminal stretch on the stability of the His−$N_{term}$ form. The study demonstrated that the stability of the His−$N_{term}$ form is significantly affected by the length of the N-terminal stretch and the N-terminal amino acid residue.

## Materials and Methods

**Protein Preparation.** The wild-type HT and PA, and the mutants were produced using *Escherichia coli* and purified as reported previously.[48,49] The oxidized proteins were prepared by the addition of a 10-fold molar excesses of potassium ferricyanide. For NMR samples, the proteins were concentrated to about 1 mM in an ultrafiltration cell (YM-5, Amicon), and then 10% $^2H_2O$ was added to the protein solutions. GdnHCl was obtained as a powder from MP Biomedicals and used without purification. For the NMR measurements, GdnHCl-$d_6$ (Cambridge Isotopes) was used as received. The pH of the sample was adjusted using 0.2 M KOH or 0.2 M HCl, and the pH was monitored with a Horiba F-22 pH meter with a Horiba type 6069-10C electrode. The pH meter has been shown to underestimate the pH value of a bulk solution in the presence of a high salt concentration. A [GdnHCl]-dependent pH correction factor (ΔpH) has been shown to be described by the following empirical equation.[50]

$$\Delta pH = -0.182 \times [GdnHCl]^{1/2} + 0.161 \times [GdnHCl] + 0.0055 \times [GdnHCl]^2$$

**Peptide Synthesis.** The amino acid residues used for the synthesis were of the *L*-configuration, and purchased from Millipore Inc. The $N^{\alpha}$-amino group was protected exclusively with a 9-fluorenylmethoxycarbonyl (Fmoc) group.[51,52] The side chain functional groups were protected as follows: a *t*-butyl group for Asp and Glu; a *t*-butyloxycarbonyl group for Lys; and a triphenylmetyl group for Asn and Gln. The peptide fragments were synthesized by means of solid-phase methodology on a Perseptive Biosystems 9050 peptide synthesizer. To prepare peptide fragments, $N^{\alpha}$-(9-fluorenylmethoxycarbonyl)-glycine *p*-alkoxylbenzyl alcohol polyethyleneglycol-modified polystyrene resin[53] (0.51 mmol Gly per gram resin, Watanabe Chemical Industries Inc.) was used. After deprotection of the N-terminal Fmoc group with 20% piperidine in *N*,*N*-dimethylformamide, in order to obtain peptides with the desired sequences, each derived amino acid residue was coupled successively in the presence of *O*-(7-azabenzotriazol-1-yl)-1,1,3,3-tetramethyluronium hexafluorophosphate[54] on the resin.

The obtained peptide-resin was treated with a mixture consisting of 0.6 mL *m*-cresol, 3.6 mL thioanisol, and 25.8 mL trifluoroacetic acid at room temperature for 2 h to cleave the peptide from the resin as well as to deprotect the side-chain functional groups. To the brown filtrate of the reaction mixture was added 70 mL of diethyl ether to give a precipitate in an ice bath. The precipitate obtained on filtration was washed with diethyl ether several times and then dissolved in 0.5 M acetic acid. The obtained solution was lyophilized to give ∼150 mg of product, which was used for NMR measurement without further purification because of the higher purity than 95% on reversed-phase high-performance liquid chromatography (RP-HPLC).

RP-HPLC was performed using a 5 μm particle size, 0.46 × 24 cm Lichrospher 100 RP-18 column (Merck) with a 0.46 × 1 cm RP-18 guard column (Merck) on a liquid chromatography system composed of a JUSCO-880 pump and a JUSCO-875 UV detector. Two isocratic solvent systems, mixtures of 0.1% trifluoroacetic and acetonitrile in different ratios (15% and 35% acetonitrile), were used to elute the peptides at a flow rate of 0.5 mL/min and the effluent was detected as to UV absorption at 210 nm.

The molecular weights (MW) of synthesized peptides were measured with a QStar Plusar i (Applied Biosystems). The experimental settings for the electron spray ionization (ESI) mass spectrometry were optimized automatically. The results were processed using the AnalystQS software attached to the instrument. Each sample were dissolved in distilled water to the concentration of ∼10 μM and then injected directly into the ESI source with a syringe pump at a flow rate of 5 μL/min. Full mass spectra were acquired in the positive ionization mode over the *m*/*z* 100−1000 range. For example, in the case of P(PA-E1N), two major ions were observed at *m*/*z* 420.9 and 630.8, which indicated $Z = 3$ and 2, respectively (see Supporting Information). The experimentally observed MWs were equal to the theoretically calculated values of the corresponding peptides.

**$^1$H NMR Spectroscopy.** NMR spectra were recorded on a Bruker Avance-600 FT NMR spectrometer operating at a $^1$H frequency of 600 MHz. Chemical shifts are given in ppm downfield from sodium 4,4-dimethyl-4-silapentane-1-sulfonate with $H_2O$ as an internal reference. Saturation transfer (ST) experiments are

(46) Travaglini-Allocatelli, C.; Gianni, S.; Dubey, V. K.; Borgia, A.; de Matteo, A.; Bonivento, D.; Cutruzzolà, F.; Bren, K. L.; Brunori, M. *J. Biol. Chem.* **2005**, *280*, 25729–25734.
(47) Matsuura, Y.; Takano, T.; Dickerson, R. E. *J. Mol. Biol.* **1982**, *156*, 389–409.
(48) Hasegawa, J.; Yoshida, T.; Yamazaki, T.; Sambongi, Y.; Yu, Y.; Igarashi, Y.; Kodama, T.; Yamazaki, K.; Kyogoku, Y.; Kobayashi, Y. *Biochemistry* **1998**, *37*, 9641–9649.
(49) Hasegawa, J.; Uchiyama, S.; Tanimoto, Y.; Mizutani, M.; Kobayashi, Y.; Sambongi, Y.; Igarashi, Y. *J. Biol. Chem.* **2000**, *275*, 37824–37826.
(50) Garcia-Mira, M. M.; Sanchez-Ruiz, J. M. *Biophys. J.* **2001**, *81*, 3489–3502.
(51) Carpino, L. A. *Acc. Chem. Res.* **1987**, *20*, 401–407.
(52) Carpino, L. A.; Han, G. Y. *J. Org. Chem.* **1972**, *37*, 3404–3409.
(53) Wang, S. S. *J. Am. Chem. Soc.* **1973**, *95*, 1328–1333.
(54) Carpino, L. A. *J. Am. Chem. Soc.* **1993**, *115*, 4397–4398.

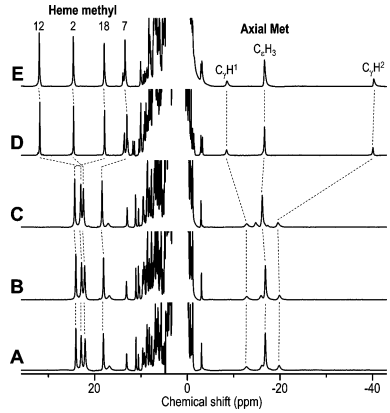


**Figure 1.** 600 MHz $^1$H NMR spectra of the oxidized forms of *Hydrogenobacter thermophilus* cytochrome $c_{552}$ (HT) (A), the N1E mutant (HT-N1E) of HT (B), an HT mutant (HT-2GG3) possessing two extra Gly residues between E2 and Q3 (C), the E1N mutant (PA-E1N) of *Pseudomonas aeruginosa* cytochrome $c_{551}$ (PA) (D), and PA (E) in 20 mM potassium phosphate buffer, pH 7.00, at 25 °C. The assignments[60,61] of the heme methyl and axial Met proton signals are indicated with the spectra and the corresponding signals in the different spectra are connected by a broken line. The heme methyl and axial Met proton signals of HT and PA were not affected by the mutations introduced, indicating that the heme active sites in the proteins were not affected by the mutations.

carried out by selectively saturating a desired peak for 40 ms, together with the recycle time of 200 ms, and the resulting spectra were presented in the form of a difference spectrum.

**pH Titration of Denatured Proteins.** Absorption spectra of 5 $\mu$M proteins were recorded on a Beckman DU 640 spectrophotometer. Cleavage of the Fe−$N_{term}$ bond of the His−$N_{term}$ form with decreasing pH was monitored at 25 °C through the pH dependence of the 399.5 nm absorbance ($A_{399.5}$), and then the results were fitted to the following equation to yield the p$K_3$ value[33−36,44]

$$A_{399.5} = \{A_{399.5,LS} + A_{399.5,HS}[10^{n(pK_3-pH)}]\}/[1 + 10^{n(pK_3-pH)}]$$

where $A_{399.5,\ LS}$ and $A_{399.5,\ HS}$ are the 399.5 nm absorbance of the LS form, i.e., the His−$N_{term}$ form, and the HS form resulting from the loss of the Fe−$N_{term}$ bond, respectively, and $n$ is the number of protons involved in the process.

## Results

**$^1$H NMR Spectra of Wild-Type and Mutant Proteins.** We first analyzed the effects of the amino acid substitutions on the heme electronic structure of the protein by paramagnetic $^1$H NMR. The 600 MHz $^1$H NMR spectra of the oxidized forms of PA, HT, and the mutants are compared with each other in Figure 1. In the $^1$H NMR spectra of the oxidized cyt *c*, heme methyl and Fe-bound Met proton signals were resolved in the downfield- and upfield-shifted regions, respectively, and have been shown to be sensitive to the heme electronic structure and coordination structure.[55−59] Differences in the heme methyl proton shift pattern

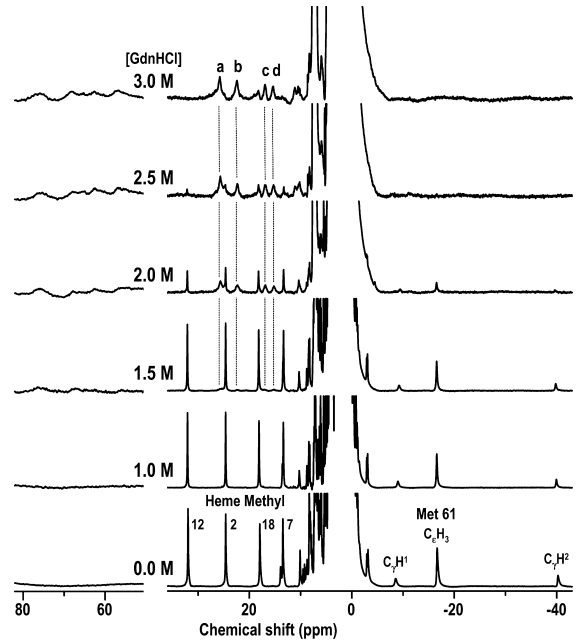


**Figure 2.** 600 MHz $^1$H NMR spectra of oxidized PA, p$^2$H 7.00, in the presence of various [GdnHCl] (0−3.0 M) at 25 °C. The assignments[61] of the heme methyl and axial Met proton signals of PA are indicated in the spectra. A new set of heme methyl proton signals, peaks a−d and signals in 50−80 ppm, emerged and their intensities increased at the expense of the native signals with increasing [GdnHCl].

and spread between PA and HT have been attributed to the difference in the orientation of the axial Met side chain, with respect to heme, between them.[58] On the other hand, the paramagnetic shift patterns of heme and axial Met methyl proton signals in the spectra of the oxidized HT-N1E and HT-2GG3 were similar to that of the wild-type HT,[60] and those of wild-type PA[61] and PA-E1N were similar to each other, indicating that the heme active site structures in the proteins are essentially unaltered by the mutations.

**Detection of the His−$N_{term}$ Form Emerging upon GdnHCl-Induced Unfolding of Oxidized PA.** We next characterized the nonnative heme coordination species emerging upon GdnHCl-induced unfolding of oxidized PA at pH 7.0 by paramagnetic $^1$H NMR. As shown in the 600 MHz $^1$H NMR spectra of the protein in the presence of various concentrations of GdnHCl ([GdnHCl]) (Figure 2), the intensities of heme methyl proton signals of native form decreased with increasing [GdnHCl], and vanished at [GdnHCl] = ∼3 M, although the shifts were only slightly affected by [GdnHCl]. At the same time, two sets of signals newly emerged at [GdnHCl] ≥ 1.5 M, and their intensities increased with increasing [GdnHCl]. One set comprises the signals emerging in the shift range characteristic of high spin (HS) ferriheme species, i.e., downfield of 50 ppm, and the other, peaks a−d, in the shift range characteristic of low-spin (LS) ferriheme species, i.e., 10−30 ppm.[59] The HS species resulting from cleavage of the Fe−Met bond in the denatured protein have been shown to be rapidly interconverted to each other through cleavage/formation of the

(55) Shokhirev, N. V.; Walker, F. A. *J. Biol. Inorg. Chem.* **1998**, *3*, 581–594.
(56) Tsan, P.; Caffrey, M.; Daku, M. L.; Cusanovich, M.; Marion, D.; Gans, P. *J. Am. Chem. Soc.* **2001**, *123*, 2231–2242.
(57) Yamamoto, Y.; Nanai, N.; Chûjô, R.; Suzuki, T. *FEBS Lett.* **1990**, *264*, 113–116.
(58) Tachiiri, N.; Hemmi, H.; Takayama, S. J.; Mita, H.; Hasegawa, J.; Sambongi, Y.; Yamamoto, Y. *J. Biol. Inorg. Chem.* **2004**, *9*, 733–742.
(59) Yamamoto, Y. *Annu. Rep. NMR Spectrosc.* **1998**, *36*, 1–77.
(60) Detlefsen, D. J.; Thanaval, V.; Pecoraro, V. L.; Wagner, G. *Biochemistry* **1991**, *30*, 9040–9046.
(61) Timkovich, R.; Cai, M. *Biochemistry* **1993**, *32*, 11516–11523.

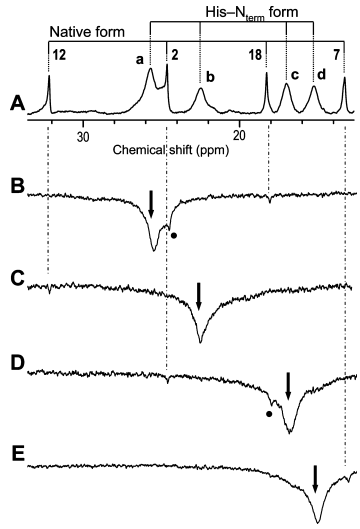


**Figure 3.** 600 MHz $^1$H NMR spectrum and saturation transfer (ST) difference spectra of oxidized PA, p$^2$H 7.40, in the presence of [GdnHCl] = 2.0 M at 25 °C. Under these conditions, both the native and His−N$_{term}$ forms of the protein coexist. The assignments[61] of the heme 12-, 2-, 18-, and 7-methyl proton signals of the native protein are indicated with the spectrum. (A) Reference spectrum. (B) ST difference spectrum on saturation of the methyl proton signal at ∼26 ppm, peak a, revealed an ST effect to the 18-Me signal of the native protein. (C) ST difference spectrum on saturation of the methyl proton signal at ∼22.5 ppm, peak b, revealed an ST effect to the 12-Me signal of the native protein. (D) ST difference spectrum on saturation of the methyl proton signal at ∼17 ppm, peak c, revealed an ST effect to the 18-Me signal of the native protein. (E) ST difference spectrum on saturation of the methyl proton signal at ∼15 ppm, peak d, revealed an ST effect to the 7-Me signal of the native protein. In (B)−(E), the saturated peak is indicated by an arrow. The observed ST connectivities led to the heme methyl proton assignments of peaks a−d to the heme 18-, 12-, 2-, and 7-Me protons, respectively.

Fe−$H_2O$ coordination bond,[23] and, as illustrated in Scheme 1, the appearance of the HS species is highly pH-dependent. The nonnative LS species has been attributed to the His−N$_{term}$ form, on chemical modification as previously described for the system of HT[24] (see Supporting Information). These results indicated that homologous PA and HT are highly alike in terms of the formation of nonnative heme coordination structures under denaturing conditions.

The newly emerging methyl proton signals, peaks a−d, were assigned on the basis of the observation of saturation transfer (ST) connectivities through ligand exchange[62] (Figure 3). In the presence of [GdnHCl] = 2.0 M, both the native and His−N$_{term}$ forms of the protein coexist (Figure 3A). Saturation of peak a yielded the ST connectivity to the heme 18-methyl proton signals of the native form (Figure 3B). Similarly, saturation of peaks b, c, and d yielded the ST connectivities to the heme 12-, 2-, and 7-methyl proton signals of the native form, respectively (Figure 3C−E). These results unambiguously indicated that peaks a−d can be assigned to the heme 18-, 12-, 2-, and 7-methyl proton signals of the His−N$_{term}$ form of the protein, respectively. The heme methyl proton shift pattern of 7 < 2 < 12 < 18, in order of increasing shift, for the His−N$_{term}$ form of PA was different from that of HT,[24] i.e., 12 < 2 < 18 < 7, but was identical to those of His-Lys coordination of horse heart cyt *c*[27,28]

(62) Yamamoto, Y.; Inoue, Y.; Suzuki, T. *Magn. Reson. Chem.* **1993**, *31*, S8–S16.

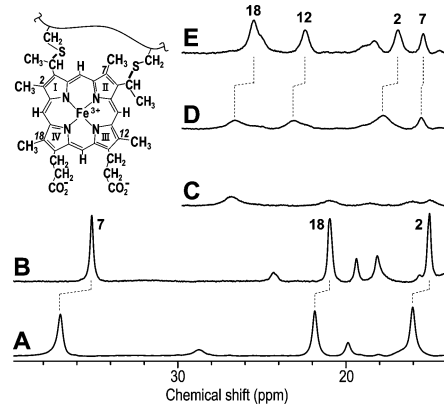


**Figure 4.** Downfield-shifted portions of 600 MHz $^1$H NMR spectra of the His−N$_{term}$ forms of HT at p$^2$H7.0 (A), HT-N1E at p$^2$H 7.0 (B), HT-2GG3 at p$^2$H 7.0 (C), PA-E1N at p$^2$H 8.0 (D), and PA at p$^2$H 8.0 (E) in the presence of [GdnHCl-$d_6$] = 6.0 M at 25 °C. The molecular structure of and numbering system for heme are illustrated in the inset. The assignments of the heme methyl proton signals of HT and PA are indicated in the spectra and the corresponding signals in the different spectra are connected by a broken line.

and yeast iso-1-cyt *c*.[29] Since the signals for both the native and His−N$_{term}$ forms were separately observed in the NMR spectra (Figures 2 and 3), the time scale of the interconversion between them was found to be slower than the NMR time scale, and a value of $\sim 1 \times 10^3$ s$^{-1}$ was estimated to be the upper limit of the interconversion rate from the difference in the resonance frequency between the signals of the two species; i.e., the chemical shift difference of ∼2 ppm between their heme 7-methyl proton signals corresponds to ∼1200 Hz at a $^1$H frequency of 600 MHz.

**Effects of the N-Terminal Stretch on the Heme Electronic Structure of the His−N$_{term}$ Form.** We also characterized the heme electronic structures of the oxidized forms of the His−N$_{term}$ forms through analysis of their paramagnetic $^1$H NMR spectra (Figure 4). Despite the fact that the heme methyl proton shift pattern of the native form of HT-2GG3 is essentially identical to that of the wild-type HT (Figure 1), the spectral pattern of the His−N$_{term}$ form of HT-2GG3 was similar to that of PA rather than that of HT. This result indicated that the heme electronic structure of the His−N$_{term}$ form is greatly affected by the length of the N-terminal stretch.

On the other hand, the heme methyl proton signals of the His−N$_{term}$ form of HT-N1E exhibited downfield shifts of 0.91−1.84 ppm at 25 °C relative to the corresponding signals of HT. Such N-terminal residue-dependent shifts were also observed between the spectra of the denatured PA and PA-E1N. These results unequivocally indicated the coordination of the N-terminal amino group to the heme Fe in the nonnative LS form, i.e., formation of the His−N$_{term}$ form. In addition, the signals emerging in the shift range characteristic of HS ferriheme species, i.e., downfield of 50 ppm, has been observed in the all denatured proteins at p$^2$H 7.0, but the concentration of the HS ferriheme species is highly pH-dependent and hence is different from each other (see Supporting Information).

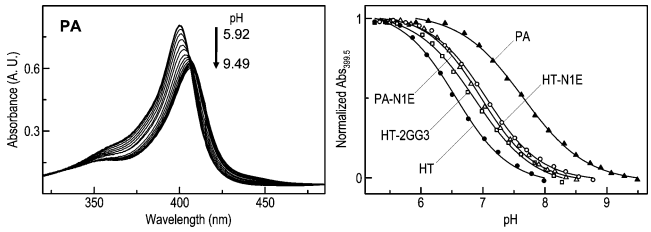


**Figure 5.** Soret absorption of oxidized PA in the presence of [GdnHCl] = 6.0 M at 25 °C and the pH range between 5.92 and 9.49 (left), and plots of the normalized 399.5 nm absorbance of HT, HT-N1E, HT-2GG3, PA, and PA-E1N as a function of pH (right). The conversion of the heme Fe spin state from low spin to high spin due to cleavage of the Fe−$N_{term}$ bond at lower pH values is reflected by the decrease in the absorbance.

**Determination of the $K_3$ Values.** Since cleavage of the Fe−$N_{term}$ bond accompanies a change in the spin state of heme Fe, this process can be readily and sensitively detected through observation of the Soret absorption band (Figure 5).[33−36,44] The p$K_3$ values obtained on fitting of the data to the Henderson−Hasselbalch equation are summarized in Table 1. The p$K_3$ values of the present proteins varied in the range of almost a pH unit, i.e., 6.66 ± 0.06 and 7.60 ± 0.03 for HT and PA, respectively. The obtained values were greatly different from those reported for the His−$N_{term}$ forms of mutants of yeast iso-1-cyt *c* possessing a 18-residue N-terminal stretch with the N-terminal Thr, i.e., p$K_3$ = ∼5.9.[33] These results suggested that the p$K_3$ value is affected by the sequence and the number of constituent amino acid residues of the N-terminal stretch. In fact, comparison of the p$K_3$ values between HT and HT-N1E, PA and PA-E1N, and HT and HT-2GG3 clearly demonstrated that the value is greatly affected by the N-terminal residue and the length of N-terminal stretch, in such a fashion that the His−$N_{term}$ form with an N-terminal Glu always exhibits a larger p$K_3$ value than that with an N-terminal Asn, and that, with a given N-terminal residue, the p$K_3$ value is larger for a 11-residue N-terminal stretch than an 9-residue one. These relatively large effects of the structural properties of the N-terminal stretch on the p$K_3$ value confirmed the formation of the His−$N_{term}$ form.

**Estimation of the $K_1$ Values.** In order to estimate the $K_1$ values of the proteins, we synthesized peptides of which the amino acid sequences are identical to those of the N-terminal stretches of the proteins under consideration. The p$K_a$ values of the N-terminal amino groups of the peptides in [GdnHCl] = 6.0 M were determined from the pH-dependent profiles of the $C_\alpha$H or $C_\beta$H proton shifts of the N-terminal residues (see Supporting Information), as summarized in Table 1. The obtained values were not significantly affected by the amino acid sequence, but were by the N-terminal residue. The p$K_a$ values for an N-terminal Glu were greater by more than a pH unit than those for an N-terminal Asn. The higher p$K_a$ value for N-terminal Glu can be attributed to the formation of the intraresidue hydrogen bond between the amino group and the side chain carboxylate.[63] It is assumed that these p$K_a$ values can be represented as the p$K_1$ values, as shown in Scheme 1.

(63) Bundi, A.; Wüthrich, K. *Biopolymers* **1979**, *18*, 299–311.

**Stability of the Fe−$N_{term}$ Bond.** With the assumption that the p$K_a$ values of the N-terminal amino groups of the model peptides are equal to the p$K_1$ values of the corresponding N-terminal stretches of the proteins, the p$K_2$ values were calculated, as shown in Table 1. Negative p$K_2$ values reflected the stability of the Fe−$N_{term}$ bond. The pattern of HT-N1E < HT < PA < PA-E1N ∼ HT-2GG3, in order of increasing the p$K_2$ value, indicated that the stability of the Fe−$N_{term}$ bond depends on both the length of the N-terminal stretch and the N-terminal residue. With a given N-terminal residue, the stability of the Fe−$N_{term}$ bond is higher for a 9-residue N-terminal stretch than an 11-residue one.[44] On the other hand, with a given length of the N-terminal stretch, the stability of the Fe−$N_{term}$ bond was higher for an N-terminal Glu than an N-terminal Asn. Furthermore, the almost identical p$K_2$ values for PA-E1N and HT-2GG3 demonstrated that, in the case of an 11-residue N-terminal stretch, the stability of the Fe−$N_{term}$ bond is independent of the amino acid sequence.

## Discussion

**Heme Electronic Structure of the His−$N_{term}$ Form.** The heme electronic structure of the His−$N_{term}$ form is significantly affected by both the axial His and N-terminal amino group coordination bonds, i.e., the Fe−His and Fe−$N_{term}$ bonds, respectively, and is sharply reflected in the paramagnetic shifts of the heme peripheral methyl proton signals.[55−59] Since the orientation of the axial His imidazole, with respect to the heme, is greatly restricted even in a denatured protein due to the presence of the heme−protein covalent linkage, together with the Fe−His bond,[23] the differences in the heme methyl proton paramagnetic shift pattern among the proteins can be primarily interpreted in terms of the Fe−$N_{term}$ bond. As shown in Figure 4, the shift patterns of the His−$N_{term}$ forms of HT and HT-N1E are similar to each other, demonstrating the similarity in the Fe−$N_{term}$ bond between them. Such similarity was also observed between the spectra of the His−$N_{term}$ forms of PA and PA-E1N. The relatively small effect of the N-terminal residue mutation on the heme methyl proton shift pattern of the His−$N_{term}$ form indicated that the heme electronic structure was not so significantly affected by the mutation. On the other hand, the distinct difference in the shift pattern between the HT and PA proteins demonstrated that the Fe−$N_{term}$ bond is greatly affected by the length of the N-terminal stretch. This conclusion was confirmed by the fact that the spectrum of the His−$N_{term}$ form of HT-2GG3 is rather similar to those of the PA proteins (Figure 4), although, in the native state, HT-2GG3 gave a spectrum essentially identical to those of the other two HT proteins, i.e., HT and HT-N1E (Figure 1). Since the coordination of the pseudo-$C_3$ symmetric $sp^3$ nitrogen atom of the N-terminal amino group to heme Fe is expected to induce small asymmetry in the unpaired electron spin delocalization of the heme,[55] relatively low dispersion of the heme methyl proton signals of ∼10 ppm was observed for PA, PA-E1N, and HT-2GG3 (see Figure 4). In fact, the heme methyl proton shift patterns of PA, PA-E1N, and HT-2GG3 were remarkably similar to those of the cylindrically

**Table 1.** Equilibrium Constants, $K_1-K_3$, of the Reactions Associated with the Formation of the His$-N_{term}$ Form of a Denatured Cyt *c* in the Presence of [GdnHCl] = 6.0 M at 25 °C

| cyt c | N-terminal amino acid | p$K_1$[a] | p$K_3$[b] | p$K_2$[c] | $\Delta\Delta G$ (kJ/mol)[d] |
|---|---|---|---|---|---|
| HT | Asn | 7.50 ± 0.02 | 6.66 ± 0.06 | −0.90 ± 0.06 | − |
| HT-N1E | Glu | 8.40 ± 0.03 | 7.06 ± 0.03 | −1.36 ± 0.04 | +2.6 ± 0.4 |
| HT-2GG3 | Asn | 7.46 ± 0.03 | 6.86 ± 0.03 | −0.70 ± 0.04 | −1.1 ± 0.4 |
| PA-E1N | Asn | 7.51 ± 0.04 | 6.91 ± 0.04 | −0.69 ± 0.05 | −0.8 ± 0.3 |
| PA | Glu | 8.36 ± 0.03 | 7.60 ± 0.03 | −0.83 ± 0.04 | − |

[a] The $K_1$ value was assumed to be equal to the p$K_a$ value of the N-terminal amino group of the corresponding model peptide. [b] The $K_3$ value was obtained through the pH dependence of the absorption spectra. [c] The $K_2$ value was calculated using $K_2 = 1 + (K_3/K_1)$. [d] The net stabilization of the His$-N_{term}$ form of the mutants relative to that of the corresponding wild-type proteins.

symmetric $CN^-$ adducts of the wild-type PA and HT in the native state, i.e., 7 < 2 < 12 < 18, in order of increasing shift of heme methyl proton signals.[58] On the other hand, the relatively great dispersion of the heme methyl proton signals of the His$-N_{term}$ forms of HT and HT-N1E, i.e., ∼30 ppm, reflected the lower symmetry of the unpaired electron spin delocalization in their hemes. These different effects of the Fe$-N_{term}$ bond on the heme electronic structures of the proteins indicated that the coordination of the $N_{term}$ atom to heme Fe depends on the length of the N-terminal stretch (see below).

**Structure and Stability of the Fe$-N_{term}$ Bond.** The greater dispersion of the heme methyl proton signals for the His$-N_{term}$ forms with a 9-residue N-terminal stretch than those with an 11-residue one indicated that the heme electronic structure of the former is more greatly distorted from pseudo-$C_4$ symmetry than the latter. In hexacoordinated LS ferriheme species, the energy levels for the $d_\pi$ ($d_{xz}$ and $d_{yz}$) orbitals are affected by the interaction with axial ligands, and a single unpaired electron resides in either the $d_{xz}$ or $d_{yz}$ orbital, whichever possesses the highest energy.[59] In the case of the His$-N_{term}$ form with a 9-residue N-terminal stretch, a single unpaired electron was found to reside primarily in the $d_\pi$ orbital, of which lobes are pointing toward the pyrrole $N_{II}$ and $N_{IV}$ atoms (see the heme structure in Figure 4), possibly due to the Fe$-N_{term}$ coordination structure. Consequently, the Fe$-N_{term}$ bond in the His$-N_{term}$ form with a 9-residue N-terminal stretch appeared to be tilted away from the heme normal so as to destabilize the $d_\pi$ orbital oriented along the $N_{II}-Fe-N_{IV}$ axis relative to the other $d_\pi$ orbital. Thus, the Fe$-N_{term}$ bond in the His$-N_{term}$ form with a 9-residue N-terminal stretch is forced to be tilted away from the heme normal. On the other hand, the Fe$-N_{term}$ bond in the His$-N_{term}$ form with an 11-residue stretch appeared to be nearly parallel with the heme normal.

In paramagnetic heme complexes, the relaxation process for heme peripheral side chain protons has been shown to be determined by the electron spin−lattice relaxation time ($T_{1e}$), which is closely related to the symmetric nature of the ligand field around the heme Fe.[59] The observation of the narrower signals for the His$-N_{term}$ forms with a 9-residue N-terminal stretch than those with an 11-residue one is consistent with lower symmetry in the ligand field in the former, as manifested in the greater heme methyl proton shift spread. This interpretation was supported by the measurements of the spin−lattice relaxation time ($T_1$), which indicated that heme methyl protons of the His$-N_{term}$ forms with a 9-residue N-terminal stretch exhibited considerably longer $T_1$ values than those of the His$-N_{term}$ forms with an 11-residue one, i.e., ∼50 and ∼10 ms for the former and the latter, respectively (see Supporting Information). But, since the ratio between the line widths of heme methyl proton signals of the two His$-N_{term}$ forms, i.e., ∼3, calculated from the values of ∼100 to ∼150 and ∼300 to ∼500 Hz for the signals of the His$-N_{term}$ forms with a 9-residue N-terminal stretch and an 11-residue one, respectively, was not equal to the value estimated from their $T_1$ values, i.e., ∼5, contributions of exchange broadening and static heterogeneity to the line widths of the signals could not be ruled out. In fact, the differences in the line widths of heme methyl proton signals among the His$-N_{term}$ forms with an 11-residue N-terminal stretch (Figure 4C−E) are likely to be attributed to differences in the contributions of exchange broadening and static heterogeneity among them.

The stability of the Fe$-N_{term}$ bond is directly reflected in the p$K_2$ value. The results demonstrated that, with a given N-terminal residue, the stability of the Fe$-N_{term}$ bond is higher for a 9-residue N-terminal stretch than an 11-residue one, and that, with a given length of the N-terminal stretch, the stability of the Fe$-N_{term}$ bond is higher for N-terminal Glu than N-terminal Asn. Comparison of the p$K_2$ values indicated that the Fe$-N_{term}$ bonds with an N-terminal Glu are stabilized by $\Delta\Delta G$ values of 2.6 ± 0.4 and 0.8 ± 0.3 kJ $mol^{-1}$ relative to those with an N-terminal Asn for HT and PA proteins, respectively (Table 1). The high stability of the Fe$-N_{term}$ bond with the N-terminal Glu might be attributed to the intraresidue hydrogen bond,[63] together with the electrostatic attraction between the side chain carboxylate and the positively charged heme Fe. Thus NMR and optical characterization of the His$-N_{term}$ forms of the denatured cyts *c* showed that the stability of the Fe$-N_{term}$ bond is significantly affected by the length of the N-terminal stretch as well as the N-terminal residue.

**Implication of the Formation of the His$-N_{term}$ Form for Protein Folding/Unfolding.** Since the values of ∼36.0 and ∼20.4 kJ $mol^{-1}$ were obtained for the energy changes ($\Delta G_U$) for GdnHCl-induced unfolding of the oxidized HT[64] and PA,[65] respectively, the differences in the stability between the His$-N_{term}$ form with an N-terminal Glu and that with an N-terminal Asn for a given protein, i.e., the $\Delta\Delta G$

(64) Hasegawa, J. Ph.D. Thesis, University of Tokyo, 2002.
(65) Hasegawa, J.; Shimahara, H.; Mizutani, M.; Uchiyama, S.; Arai, H.; Ishii, M.; Kobayashi, Y.; Ferguson, S. J.; Sambongi, Y.; Igarashi, Y. *J. Biol. Chem.* **1999**, *274*, 37533–37537.

values of 2.6 ± 0.4 and 0.8 ± 0.3 kJ mol$^{-1}$ for HT and PA, respectively, change the $\Delta G_U$ value by 4−7%. Thus, the stability of the His−$N_{term}$ form makes a certain contribution to the overall protein stability, although the N-terminal amino acid residue has been thought to contribute very little to it.

The formation of the His−$N_{term}$ form is also expected to affect the pathway and kinetics of the folding/unfolding of cyts *c*, of which the N-terminal amino groups are not acetylated. The pairing of two helices at opposite ends of the polypeptide chain is a highly conserved structural motif found in the cyt *c* family, and the association of the N- and C-terminal helices has been shown to accompany the first step of usual cyt *c* folding.[12−14] Further folding is prevented at this stage due to the formation of nonnative heme coordination structures such as the *bis*-His form.[38−43] Since the coordination of the N-terminal amino group to heme Fe upon the formation of the His−$N_{term}$ form results in prohibition of the N-terminal helix formation, which in turn hampers the bihelical association critical for initiation of the protein folding, the mechanism of the folding/unfolding of the proteins possessing non-acetylated N-terminal amino groups is likely to be different from that of those with acetylated N-terminal residues, as reported previously.[33,37]

## Conclusion

Characterization of residual structures in protein-denatured states is an important task for elucidating the folding/unfolding mechanisms of proteins. In this study, we have characterized the heme Fe coordination structures and stabilities of the His−$N_{term}$ forms emerging, as a residual structure upon GdnHCl-induced unfolding of the oxidized forms of HT, PA, and their mutants. The results here clearly indicated that the His−$N_{term}$ form is considerably stable, and that the stability of the His−$N_{term}$ form is significantly afected by the length of the N-terminal stretch and the N-terminal residue. These findings provide a novel insight into the stabilizing interactions in denatured cyts *c*, possessing non-acetylated N-terminal amino groups, that will facilitate elucidation of the folding/unfolding mechanisms of the proteins.

**Acknowledgment.** We thank Dr. Yoshihiro Sambongi (Hiroshima University) for the gift of the proteins. This work was supported by a research grant from MEXT, the Yazaki Memorial Foundation for Science and Technology, and the NOVARTIS Foundation (Japan) for the Promotion of Science.

**Supporting Information Available:** The results from the amino acid analysis of Lys side-chain amino group modified HT (*Har*-HT) and N-terminal amino group modified HT ($N_{keto}$-HT), and the downfield-shifted portions of 600 MHz $^1$H NMR spectra of *Har*-HT, oxidized HT, and $N_{keto}$-HT, in the presence of [GdnHCl] = 6.0 M, at 25 °C and p$^2$H 7.00, the results from the amino acid analysis of N-terminal amino group modified PA ($N_{keto}$-PA), and the downfield-shifted portions of 600 MHz $^1$H NMR spectra of $N_{keto}$-PA and oxidized HT, in the presence of [GdnHCl] = 2.0 or 4.0 M, at 25 °C and p$^2$H 7.40 or 7.80, 600 MHz $^1$H NMR spectra of HT-N1H, in the presence of [GdnHCl] = 6.0 M, at 25 °C and various p$^2$H values, 4.49−9.32, 600 MHz $^1$H NMR spectra of the His−$N_{term}$ forms of HT, HT-N1E, HT-2GG3, PA-E1N, and PA in the presence of [GdnHCl-$d_6$] = 6.0 M at 25 °C and p$^2$H 7.00, the Soret absorption of oxidized HT, HT-N1E, HT-2GG3, and PA-E1N in the presence of [GdnHCl] = 6.0 M, at 25 °C and the p$^2$H range from 5.2 to 9.0, the amino acid analysis of the synthesized peptides, the molecular weights of the synthesized peptides, 600 MHz $^1$H NMR spectra of the synthesized peptides, the $^1$H NMR signal assignments for the synthesized peptides, the pH dependence of portions of 600 MHz $^1$H NMR spectra of the synthesized peptides in the present of [GdnHCl] = 6.0 M, at 25 °C, pH profiles of the N-terminal $C_\alpha$H or $C_\beta$H proton shifts of the synthesized peptides in the present of [GdnHCl] = 6.0 M, at 25 °C, the results of the selective $T_1$ values of selected heme methyl proton signals of His−$N_{term}$ forms of HT and PA, and saturation transfer difference spectra of HT-2GG3, in the presence of [GdnHCl] = 6.0 M, at 25 °C and p$^2$H 7.40. This material is available free of charge via the Internet at http://pubs.acs.org.

IC801202D